Journal of Computational Applied Mechanics 2023, 54(4): 515-532

DOI: 10.22059/JCAMECH.2023.365220.876

RESEARCH PAPER

Thermoelastic analysis of rotating thick-walled cylindrical pressure vessels with linear variable thickness under bi-directional temperature

Fatemeh Ramezani [a], Mohammad Zamani Nejad [a,*], Mehdi Ghannad [b]

[a] *Department of Mechanical Engineering, Yasouj University, Yasouj, Iran*
[b] *Mechanical Engineering Faculty, Shahrood University of Technology, Shahrood, Iran*

Abstract

Using the disk-form multi-layer method (MLM), a semi-analytical thermoelastic solution for rotating thick cylindrical pressure vessels with varying thickness is obtained. The first-order shear deformation theory (FSDT) is used for displacement and bi-directional temperature fields. The thick shell is divided into some virtual disks, and then a set of differential equations for constant thickness are obtained for each virtual disk. The general solution of the thick cylindrical shell is obtained, by applying continuity conditions between the virtual disks. The governing equations, which are a system of differential equations with variable coefficients, have been solved with MLM. Finally, some numerical results are presented to study the effects of mechanical and thermal loading, on the mechanical behavior of the thick cylindrical shell.

Keywords: Thick cylindrical shell; Variable thickness; Bi-directional temperature fields; FSDT; Multi-layers method (MLM);

1. Introduction

Thick cylindrical shells with variable thickness are complex structures that require advanced analytical and computational methods for their design and analysis. The classic theories of thick wall shells have some limitations and may not accurately predict the behavior of such shells. As a result, researchers have developed more advanced analytical and semi-analytical methods for analyzing these structures [Fatehi and Nejad [1]; Mazarei et al. [2]; Nejad et al. [3]; Farajpour and Rastgoo [4]; Ebrahimi et al. [5]; Afshin et al. [6]; Kashkoli et al. [7]; Gharibi et al. [8]; Nejad et al [9]; Kashkoli et al. [10]; Jabbari and Nejad [11]; Dindarloo and Li [12]; Taghizadeh et al. [13]; Sofiyev and Fantuzzi [14]; Taghizadeh and Nejad [15]; Jabbari and Nejad [16]]. Furthermore, extensive research has been conducted in this field due to the diverse applications of these structures [kashkoli et al. [17]; Nejad et al. [18]; Kashkoli and Nejad [19]; Nejad and Fatehi [20]; Nejad and Kashkoli [21]; Dehghan et al. [22]; Kashkoli and Nejad [23]; Nejad et al.[24]; Farajpour et al. [25]; Li et al. [26]; Nejad et al. [27]; Ghannad and Nejad [28];Zhang and She [29]]. Panferov [30] utilized the successive approximations method to derive a solution to the problem of thermal loading on an elastic truncated conical pipe that has a uniform thickness. Sundarasivarao and Ganesan [31] utilized the finite element technique to investigate a conical shell that was exposed to pressure. Mirsky and Hermann [32] obtained the solution for thick cylindrical shells made of uniform and isotropic materials by utilizing the FSDT. Witt [33] obtained a differential equation for a conical shell under axis-symmetric temperature distributions. To find a specific solution for this

* Corresponding author. Tel.: +98-7431005163; fax: +98-7431005000.
E-mail address: m_zamani@yu.ac.ir ; m.zamani.n@gmail.com

equation, Witt made an assumption that the temperature distribution could be expressed as a combination of hyperbolic and cubic functions. Jane and Wu [34] conducted research on the problem of thermoelasticity using the curvilinear circular conical coordinate system. For the elastic analysis of a thick conical shell subjected to nonuniform internal pressure, Eipakchi et al. [35] employed a mathematical approach based on perturbation theory for the elastic analysis of a thick conical shell with varying thickness under non-uniform internal pressure. Ghannad et al. [36] derived an elastic solution for truncated conical shells that are thick and have a uniform thickness. Arefi and Rahimi [37] investigated the thermoelastic behavior of a cylinder made of functionally graded material (FGM) when subjected to both mechanical and thermal loads. Eipakchi [38] employed a third-order shear deformation theory along with matched asymptotic expansion (MAE) of perturbation theory to determine the displacements and stresses of a thick conical shell. The shell was assumed to be homogeneous, isotropic, and axisymmetric, with non-uniform internal pressure causing variations in thickness. Ghannad et al. [39] studied displacements and stresses in pressurized thick cylindrical shells by using perturbation technique. Civalek [40] conducted a study on the free vibration analysis of laminated conical shells. The author investigated the cases of isotropic, orthotropic, and laminated materials and used the numerical solution of governing differential equations of motion based on transverse shear deformation theory to obtain the results. Nejad et al. [41] studied analytical solution and numerical solution on truncated conical shells Due to the existence of shear stress in the truncated cone based on FSDT.

Nejad et al. [42] presented a semi-analytical solution in a rotating cylindrical shell with variable thickness under uniform pressure based on FSDT. Ghannad et al. [43] studied of elastic analysis of pressurized FGM thick cylindrical shells. Nejad et al. [44] developed a mathematical solution that partially uses analysis and partially uses numerical methods to calculate the displacements and stresses in a cylindrical shell with varying thickness under a non-uniform pressure. Ghannad et al. [45] studied a semi-analytical solution to determine displacements and stresses in a thick cylindrical shell with variable thickness under uniform pressure based on disk form multilayers by using FSDT. Xin et al. [46] introduced a thermo-elasticity solution for one-dimensional FG cylinders that is based on the constituents' volume fraction and accounts for both thermal and mechanical loads. They systematically examined how the primary factors of the problem affect displacement and stress levels. Gharooni et al. [47] obtained thermo-elastic analysis of thick FGM cylinders based on third-order shear deformation theory by using perturbation technique. Jabbari et al. [48] developed a semi-analytical solution for thermo-elastic analysis using higher-order shear deformation theory for the vessel made of FGM subjected to the temperature gradient and internal non-uniform pressure. Nejad et al. [49] studied semi-analytically a FG rotating thick hollow cylinder with variable thickness and clamped ends under arbitrarily non-uniform pressure on the inner surface by using the FSDT. Jabbari et al. [50] researched the thermoelastic analysis of a thick truncated conical shell that rotates, has a constant thickness, and is exposed to a temperature gradient and non-uniform internal pressure. Jabbari et al. [51] presented a semi-analytical solution to obtain the displacements and stresses in an FGM rotating thick cylindrical shell with clamped ends under non-uniform pressure based on FSDT. Ghannad and Nejad [52] presented an elastic solution of pressurized FGM thick cylindrical shells based on FSDT. Jabbari et al. [53] investigated a thermo-elastic analysis of a rotating truncated conical shell subjected to temperature, internal pressure, and external pressure by using the FSDT and MLM. Yasinsky and Tokova [54] conducted a study on a one-dimensional temperature transient analysis and thermal stress analysis in an FG cylinder. They derived a solution for the problem by reducing it to a reverse thermo-elasticity problem. Nejad et al. [55] presented a general formulation for thermo-elastic analysis of a FG thick shell of revolution based on higher-order shear deformation theory. Hamzah et al. [56] conducted a comprehensive study of the vibration characteristics of cylindrical shells under different ambient temperatures by using (FEM). Kashkoli [57] studied a thermomechanical solution for creep analysis of FG thick cylindrical pressure vessels with variable thickness using the FSDT and multilayer method. Aghaienezhad et al. [58] paper derived the GDQ method to analyze the behavior of spherical and cylindrical shells subjected to external pressure. Ifayefunmi and Ruan [59] presented a computational finite element study on the instability behavior of cylinder shells under axial compressive load. Ariatapeh et al. [60] analyzed stress and deformation in thick-walled cylindrical pressure vessels/pipes made of Mooney-Rivlin hyperelastic materials, presented their distributions, and evaluated the effects of various factors. Nejad et al. [61] studied elastic analysis of thick truncated conical shells under non-uniform pressure loading. Mannani et al. [62] analyzed the mechanical stress, static strain, and deformation of a cylindrical pressure vessel under mechanical loads using higher-order sinusoidal shear deformation theory and thickness stretching formulation. A parametric study investigates the stress and strain components, and the effect of the thickness stretching model is explored.

This study presents a thermo-elastic analysis of a thick cylindrical pressure vessel with variable thickness using the MLM, which is a very efficient method. The thermal distribution is as bi-directional. The FSDT is utilized to solve the problem. The results obtained are compared with those derived from the finite element method (FEM) for selected load cases.

2. Governing Equation

2.1. Mechanical analysis

In FSDT, the assumption is made that the shear strain is assumed to be constant through the thickness of the shell. This theory predicts that the sections that are straight and perpendicular to the mid-plane of the shell will remain straight after deformation, but not necessarily perpendicular.

Geometry and boundary condition and loading condition of a thick cylindrical shell with variable thickness *h*, and the length *L*, are shown in Fig. 1. The location of a typical point *m*, within the shell element is

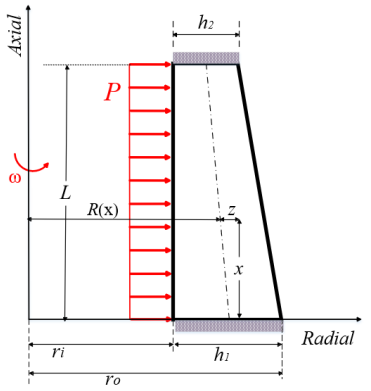

Fig. 1: Cross section of the rotating thick cylindrical pressure vessels with clamped–clamped ends

$$\begin{cases} m:(r,x)=(R+z,x) \\ 0\le x\le L \qquad \& \qquad -\dfrac{h}{2}\le z\le \dfrac{h}{2} \\ h=R_o-R_i \end{cases} \tag{1}$$

where *z* is the distance of a typical point from the middle surface. In Eq. 1, *R(x)* represents the distance of the middle surface from the axial direction and variable thickness *h* are

$$\begin{cases} R(x)=\dfrac{R_i+R_o}{2} \\ h=R_o-R_i \end{cases} \tag{2}$$

where R_o is the tapering angle as

$$R_o=R_i+h_1-(h_1-h_2)\left(\frac{x}{L}\right) \tag{3}$$

The general axisymmetric displacement field (U_x, U_z), in the FSDT could be stated based on axial displacement and radial displacement, as follows [63].

$$\begin{Bmatrix} U_x \\ U_z \end{Bmatrix}=\begin{Bmatrix} u_0(x) \\ w_0(x) \end{Bmatrix}+\begin{Bmatrix} u_1(x) \\ w_1(x) \end{Bmatrix}z \tag{4}$$

where $u_0(x)$ and $w_0(x)$ are the displacement components of the middle surface. Also, $u_1(x)$ and $w_1(x)$ are the functions used to determine the displacement field. The strain-displacement relations in the cylindrical coordinates system are [64].

$$\begin{cases} \varepsilon_x = \dfrac{\partial U_x}{\partial x} = \dfrac{du_0}{dx} + \dfrac{du_1}{dx} z \\ \varepsilon_\theta = \dfrac{U_z}{r} = \dfrac{1}{R+z}\left(w_0 + w_1 z\right) \\ \varepsilon_z = \dfrac{\partial U_z}{\partial z} = w_1 \\ \gamma_{xz} = \dfrac{\partial U_x}{\partial z} + \dfrac{\partial U_z}{\partial x} = \left(u_1 + \dfrac{dw_0}{dx}\right) + \dfrac{dw_1}{dx} z \end{cases} \tag{5}$$

Considering the effect of the thermal strain on homogenous and isotropic materials, the stress-strain relations (i.e., constitutive equations) are as follows [64].

$$\begin{bmatrix} \sigma_z \\ \sigma_\theta \\ \sigma_x \\ \tau_{zx} \end{bmatrix} = \frac{E}{(1-2\nu)(1+\nu)} \begin{bmatrix} 1-\nu & \nu & \nu & 0 \\ \nu & 1-\nu & \nu & 0 \\ \nu & \nu & 1-\nu & 0 \\ 0 & 0 & 0 & \dfrac{(1-2\nu)}{2} \end{bmatrix} \begin{bmatrix} \varepsilon_z \\ \varepsilon_\theta \\ \varepsilon_x \\ \gamma_{zx} \end{bmatrix} - \frac{E}{(1-2\nu)} \begin{bmatrix} \alpha \\ \alpha \\ \alpha \\ 0 \end{bmatrix} T \tag{6}$$

Here, σ_z, σ_θ, σ_x, τ_{zx} and ε_z, ε_θ, ε_x, γ_{zx} are the stresses and strains in the axial (x), circumferential (θ) and radial (z) directions, respectively. Also, υ, E, α and T are Poisson's ratio, modulus of elasticity, the coefficient of thermal expansion and temperature gradient, respectively.

3. Thermal Analysis

Due to the influence of $(\partial/\partial\theta) = 0$, the temperature distribution function within the cylinder can be expressed solely as a function of the radial coordinate (r) and the axial coordinate (x), therefore

$$T = T(r, x) \tag{7}$$

The temperature field for this cylinder with varying thickness using the first-order temperature theory (FTT) is expressed as follows [65]:

$$\begin{aligned} T = T(z,x) &= T(0,x) + z \left.\frac{\partial T(z,x)}{\partial z}\right|_{z=0} + \frac{z^2}{2} \left.\frac{\partial^2 T(z,x)}{\partial z^2}\right|_{z=0} + \ldots \\ &= T^0(x) + zT^1(x) = T^0 + zT^1 \end{aligned} \tag{8}$$

where, T^0 and T^1 are the zero-order and first-order components of temperature respectively, which are only a function of axial direction x.

Assuming T^* as the reference temperature, for temperature changes from the reference temperature $\Theta(z,x)$, is as follows:

$$\Theta(z,x) = T - T^* = \Theta^0(x) + z\Theta^1(x) = \Theta^0 + z\Theta^1 \tag{9}$$

where Θ^0 and Θ^1 denote the temperature variations relative to a reference temperature, specifically representing the zero-order and first-order components, respectively.

These functions are only a function of axial direction x. Using gradients relations in the cylinder coordination [66] and using Eq. (9), the thermal field-temperature variations relationships are derived, as:

$$\begin{cases} e_z = -\dfrac{\partial \Theta(x,z)}{\partial z} = -\Theta^1(x) \\ e_\theta = 0 \\ e_x = -\dfrac{\partial \Theta(x,z)}{\partial x} = -\dfrac{d\Theta^0(x)}{dx} - \dfrac{d\Theta^1(x)}{dx} z \end{cases} \tag{10}$$

where e_z, e_θ and e_x are thermal field components in the radial, circumferential, and axial directions. Also, the thermal strain and heat flux in the axisymmetric isotropic cylinder with varying thickness is calculated as follows:

$$\begin{Bmatrix} \varepsilon_z^t \\ \varepsilon_\theta^t \\ \varepsilon_x^t \\ \varepsilon_{zx}^t \end{Bmatrix} = \begin{Bmatrix} \alpha_{11} \\ \alpha_{22} \\ \alpha_{33} \\ \alpha_{13} \end{Bmatrix} \Theta \tag{11}$$

$$\begin{bmatrix} q_z \\ q_x \end{bmatrix} = \begin{bmatrix} K & 0 \\ 0 & K \end{bmatrix} \begin{bmatrix} e_z \\ e_x \end{bmatrix} \tag{12}$$

where $\varepsilon_z^t, \varepsilon_\theta^t, \varepsilon_x^t$ and ε_{xz}^t are the thermal strain. In addition, q_z and q_x are heat flux components in the radial (z) and axial (x) directions. Also, κ is the thermal conduction coefficient. The normal forces ($N_z^{m,t}$, $N_\theta^{m,t}$, $N_x^{m,t}$), bending moments($M_z^{m,t}$, $M_\theta^{m,t}$, $M_x^{m,t}$), shear force (Q_x), and the torsional moment (M_{xz}) in terms of mechanical (index *m*) and thermal (index *t*) stress resultants are [67]:

$$\begin{Bmatrix} N_z^m \\ N_\theta^m \\ N_x^m \end{Bmatrix} = \int_{-h/2}^{h/2} \begin{Bmatrix} \sigma_z(1+\frac{z}{R}) \\ \sigma_\theta \\ \sigma_x(1+\frac{z}{R}) \end{Bmatrix} dz$$

$$\begin{Bmatrix} M_\theta^m \\ M_x^m \end{Bmatrix} = \int_{-h/2}^{h/2} \begin{Bmatrix} \sigma_\theta \\ \sigma_x(1+\frac{z}{R}) \end{Bmatrix} z dz$$

$$\begin{Bmatrix} Q_x^m \\ M_{zx}^m \end{Bmatrix} = k \int_{-h/2}^{h/2} \begin{Bmatrix} 1 \\ z \end{Bmatrix} \tau_{zx} \left(1+\frac{z}{R}\right) dz$$

$$\begin{Bmatrix} N_z^t \\ N_x^t \end{Bmatrix} = \int_{-h/2}^{h/2} \begin{Bmatrix} h_z \\ h_x \end{Bmatrix} \left(1+\frac{z}{R}\right) dz$$

$$M_z^t = \int_{-h/2}^{h/2} h_x \left(1+\frac{z}{R}\right) z dz \tag{13}$$

where in k is a correction factor incorporated into the shear stress term. In the static state, for conical shells $k = 5/6$ [68].

According to the principle of virtual work, the changes in strain energy are equivalent to the changes in external work done, as expressed below [63].

$$\delta U = \delta W \tag{14}$$

where *U* is the total strain energy of the elastic body and *W* is the total work of external forces due to internal pressure and centrifugal force. By substituting strain energy and the work of external forces, we have

$$\delta U = \int_0^L \int_0^{2\pi} \int_{-h/2}^{h/2} \frac{1}{2} \begin{pmatrix} \sigma_z \delta\varepsilon_z + \sigma_\theta \delta\varepsilon_\theta + \sigma_x \delta\varepsilon_x \\ + \tau_{zx} \delta\gamma_{zx} - h_x \delta e_x - h_z \delta e_z \end{pmatrix} (R+z) dz d\theta dx \tag{15}$$

$$\partial W = \int_0^L \int_0^{2\pi} \left((P\delta U_z - H_i \delta\Theta) \left(R - \frac{h}{2}\right) + H_O \delta\Theta \left(R + \frac{h}{2}\right) \right) dx d\theta \tag{16}$$

Substituting Eqs. (15)-(16) into Eq. (14), and drawing upon the calculus of variation and the virtual work principle, concerning Eq. (13), the governing equations are obtained as:

$$\begin{cases} -\dfrac{d}{dx}\left(RN_x^m\right)=0 \\ RQ_x^m-\dfrac{d}{dx}\left(RM_x^m\right)=0 \\ RN_z^m-\dfrac{d}{dx}\left(RM_{zx}^m\right)+M_\theta^m=-P\dfrac{h}{2}\left(R-\dfrac{h}{2}\right)+\dfrac{\rho\omega^2}{6}Rh^3 \\ N_\theta^m-\dfrac{d}{dx}\left(RQ_x^m\right)=P\left(R-\dfrac{h}{2}\right)+\dfrac{\rho\omega^2}{6}\dfrac{h}{2}\left(12R^2+h^2\right) \\ -\dfrac{d}{dx}\left(RN_x^t\right)=H_0\left(R+\dfrac{h}{2}\right)-H_i\left(R-\dfrac{h}{2}\right) \\ RN_z^t-\dfrac{d}{dx}\left(RM_x^t\right)=H_i\dfrac{h}{2}\left(R-\dfrac{h}{2}\right)+H_o\left(R+\dfrac{h}{2}\right) \end{cases} \tag{17}$$

Also, the boundary conditions are

$$\frac{d}{dx}\begin{pmatrix} RN_x^m\delta u+RM_x^m\delta\varphi+RQ_x^m\delta w+RM_{zx}^m\delta\psi \\ +RN_x^t\delta\Theta^0(x)+RM_x^t\delta\Theta^1(x) \end{pmatrix}=0 \tag{18}$$

The number of thermal and mechanical resultants isn't equal to the number of equations about Eq. (17), thus for solving the set of differential Eq. (17) thermal and mechanical are required to be expressed in terms of the components of temperature and displacement field. Eq. (18) states the boundary conditions which must exist at the two ends of the cylinder. By substituting Eq. (13) into Eq. (17), the set of differential Eq. (17) may be rewritten as:

$$[A_1]\frac{d^2}{dx^2}\{\bar{y}\}+[A_2]\frac{d}{dx}\{\bar{y}\}+[A_3]\{\bar{y}\}=[F] \tag{19}$$

$$\{\bar{y}\}=\left\{\frac{du_0}{dx},u,w_0,w_1,\frac{d\Theta^0}{dx},\Theta^1\right\} \tag{20}$$

where $[A_1]_{6\times6}$, $[A_2]_{6\times6}$, $[A_3]_{6\times6}$ are the coefficients matrices, and F is the force vector, as:

$$[A_1]=\begin{bmatrix} 0 & 0 & 0 \\ 0 & -\dfrac{E(1-\nu)}{(1-2\nu)(1+\nu)}R\dfrac{h^3}{12} & 0 \\ 0 & 0 & -k\dfrac{E}{2(1+\nu)}Rh \\ 0 & 0 & -k\dfrac{E}{2(1+\nu)}\dfrac{h^3}{12} \\ 0 & 0 & 0 \\ 0 & 0 & 0 \end{bmatrix}$$

$$\begin{bmatrix} 0 & 0 & 0 \\ 0 & 0 & 0 \\ -k\dfrac{E}{2(1+\nu)}\dfrac{h^3}{12} & 0 & 0 \\ -k\dfrac{E}{2(1+\nu)}R\dfrac{h^3}{12} & 0 & 0 \\ 0 & 0 & 0 \\ 0 & R\int\limits_{-h/2}^{h/2} Kzdz & \int\limits_{-h/2}^{h/2} Kz^3dz \end{bmatrix} \tag{21}$$

$$[A_2]=\begin{bmatrix} 0 & \dfrac{E(1-\nu)}{(1-2\nu)(1+\nu)}\dfrac{h^3}{12} & 0 \\ -\dfrac{E(1-\nu)}{(1-2\nu)(1+\nu)}\dfrac{h^3}{12} & -\dfrac{(1-\nu)}{(1-2\nu)(1+\nu)}\dfrac{h^2}{12}\left(3R\dfrac{dh}{dx}+h\dfrac{dR}{dx}\right) & k\dfrac{E}{2(1+\nu)}Rh \\ 0 & -k\dfrac{E}{2(1+\nu)}Rh & -\dfrac{k}{2(1+\nu)}\left(RE\dfrac{dh}{dx}+hE\dfrac{dR}{dx}\right) \\ 0 & \dfrac{E}{(1+\nu)}\dfrac{h^3}{12}\left(\dfrac{2\nu}{(1-2\nu)}-\dfrac{k}{2}\right) & -\dfrac{kE}{2(1+\nu)}\dfrac{h^2}{4}\dfrac{dh}{dx} \\ 0 & 0 & 0 \\ 0 & 0 & 0 \end{bmatrix}$$

$$\begin{bmatrix} 0 & 0 & 0 \\ \dfrac{E}{(1+\nu)}\dfrac{h^3}{12}\left(\dfrac{k}{2}-\dfrac{\nu}{(1-2\nu)}\right) & \dfrac{E(1+\nu)}{(1-2\nu)(1+\nu)}\dfrac{h^3}{12}\alpha & \dfrac{E(1+\nu)}{(1-2\nu)(1+\nu)}R\dfrac{h^3}{12}\alpha \\ -\dfrac{kE}{2(1+\nu)}\dfrac{h^2}{4}\dfrac{dh}{dx} & 0 & 0 \\ -\dfrac{k}{2(1+\nu)}\dfrac{h^2}{12}\left(hE\dfrac{dR}{dx}+3RE\dfrac{dh}{dx}\right) & 0 & 0 \\ 0 & 0 & 0 \\ 0 & \dfrac{dR}{dx}\int\limits_{-h/2}^{h/2} Kzdz & 0 \end{bmatrix} \tag{22}$$

$$[A_3]=\begin{bmatrix}
\frac{E(1-\nu)}{(1-2\nu)(1+\nu)}Rh & 0 & \frac{E\nu}{(1-2\nu)(1+\nu)}h \\
-\frac{E(1-\nu)}{(1-2\nu)(1+\nu)}\frac{h^2}{4}\frac{dh}{dx} & k\frac{E}{2(1+\nu)}Rh & 0 \\
\frac{E\nu}{(1-2\nu)(1+\nu)}h & -\frac{kE}{2(1+\nu)}\left(R\frac{dh}{dx}+h\frac{dR}{dx}\right) & \frac{E(1-\nu)}{(1-2\nu)(1+\nu)}\ln\left(\frac{R+\frac{h}{2}}{R-\frac{h}{2}}\right) \\
\frac{E\nu}{(1-2\nu)(1+\nu)}Rh & -\frac{kE}{2(1+\nu)}\frac{h^2}{4}\frac{dh}{dx} & \frac{E}{(1-2\nu)(1+\nu)}\left(h-(1-\nu)R\ln\left(\frac{R+\frac{h}{2}}{R-\frac{h}{2}}\right)\right) \\
0 & 0 & 0 \\
0 & 0 & 0
\end{bmatrix}$$

$$\begin{bmatrix}
\frac{E\nu}{(1-2\nu)(1+\nu)}Rh & -\frac{E(1+\nu)}{(1-2\nu)(1+\nu)}Rh\alpha & -\frac{E(1+\nu)}{(1-2\nu)(1+\nu)}\frac{h^3}{12}\alpha \\
\frac{E\nu}{(1-2\nu)(1+\nu)}\frac{h^2}{2}\frac{dh}{dx} & \frac{(1+\nu)}{(1-2\nu)(1+\nu)}\frac{h^2}{12}\left(3\alpha E\frac{dh}{dx}+hE\frac{d\alpha}{dx}\right) & \frac{(1+\nu)}{(1-2\nu)(1+\nu)}\frac{h^2}{12}\left(3\alpha ER\frac{dh}{dx}+hER\frac{d\alpha}{dx}+\alpha Eh\frac{dR}{dx}\right) \\
-\frac{E}{(1-2\nu)(1+\nu)}\left(h-(1-\nu)R\ln\left(\frac{R+\frac{h}{2}}{R-\frac{h}{2}}\right)\right) & -\frac{E(1+\nu)}{(1-2\nu)(1+\nu)}h\alpha & 0 \\
\frac{E(1-\nu)}{(1-2\nu)(1+\nu)}R^3\ln\left(\frac{R+\frac{h}{2}}{R-\frac{h}{2}}\right) & -\frac{E(1+\nu)}{(1-2\nu)(1+\nu)}Rh\alpha & -\frac{E(1+\nu)}{(1-2\nu)(1+\nu)}\frac{h^3}{6}\alpha \\
0 & -R\int_{-h/2}^{h/2}Kdz & -\int_{-h/2}^{h/2}Kz^2dz \\
0 & 0 & -\int_{-h/2}^{h/2}K(R+z)dz
\end{bmatrix} \tag{23}$$

$$[F]=\begin{Bmatrix}
C_1 \\
0 \\
P\frac{h}{2}\left(R-\frac{h}{2}\right)+\frac{\rho\omega^2}{6}Rh^3 \\
-P\left(R-\frac{h}{2}\right)+\frac{\rho\omega^2}{6}\frac{h}{2}\left(12R^2+h^2\right) \\
\left[H_o\left(R-\frac{h}{2}\right)-H_i\left(R+\frac{h}{2}\right)\right]x+C_2 \\
\frac{h}{2}\left[H_i\left(R-\frac{h}{2}\right)+H_o\left(R+\frac{h}{2}\right)\right]
\end{Bmatrix} \tag{24}$$

4. Multi-Layered Method (MLM)

In the MLM, a homogeneous cylinder with a non-uniform thickness is partitioned into homogeneous disc-shaped layers with a uniform thickness of $h^{[k]}$. By the mentioned assumptions, the set of non-homogenous linear differential equations converts to a nonhomogeneous set of differential equations with constant coefficients by using the ML method that for each homogenous disc are obtained as follows.

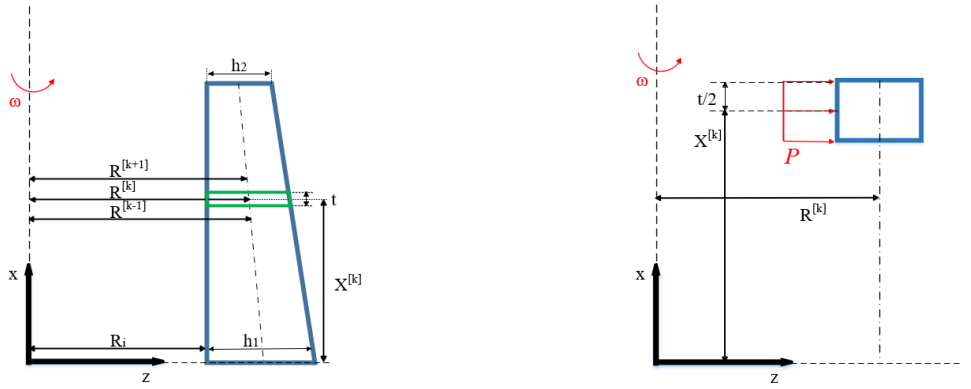

Fig. 2: Division of cylindrical shell with variable thickness to homogenous disks with constant thickness

As a result, the governing equations are transformed into a non-homogeneous set of differential equations featuring constant coefficients. $x^{[k]}$ and $R^{[k]}$ are the length and radius of the middle of the disks. The modulus of elasticity and Poisson's ratio of disks are assumed to be constant. The length of the middle of an arbitrary disk (Fig. 2) is as follows

$$\begin{cases} R^{[k]}(x)=\dfrac{R_i+R_o^{[k]}}{2} \\ h^{[k]}=R_o^{[k]}-R_i \end{cases} \tag{25}$$

where

$$R_o^{[k]}=R_i+h_1-\left(h_1-h_2\right)\left(\frac{x^{[k]}}{L}\right) \tag{26}$$

Thus

$$\left(\frac{dh}{dx}\right)^{[k]}=2\left(\frac{dR}{dx}\right)^{[k]}=\left(\frac{dR_0}{dx}\right)^{[k]} \tag{27}$$

Poisson's ratio of disks is assumed to be constant. The governing equations for each homogenous disk are derived as follows:

$$\left[A_1\right]^{[k]}\frac{d^2}{dx^2}\{\bar{y}\}^{[k]}+\left[A_2\right]^{[k]}\frac{d}{dx}\{\bar{y}\}^{[k]}+\left[A_3\right]^{[k]}\{\bar{y}\}^{[k]}=[F]^{[k]} \tag{28}$$

$$\{\bar{y}\}^{[k]}=\left\{\left(\frac{du_0}{dx}\right)^{[k]},u_1^{[k]},w_0^{[k]},w_1^{[k]},\left(\frac{d\theta^0}{dx}\right)^{[k]},\theta 1^{[k]}\right\}^T \tag{29}$$

$\left[A_i\right]_{6\times6}^{[k]}$ The coefficients matrices and $\{F\}_{6\times6}^{[k]}$ force vector are as follows:

$$\left[A_1\right]=\begin{bmatrix} 0 & 0 & 0 \\ 0 & -\frac{E(1-\nu)}{(1-2\nu)(1+\nu)}R^{[k]}\frac{h^{[k]3}}{12} & 0 \\ 0 & 0 & -k\frac{E}{2(1+\nu)}R^{[k]}{}_h{}^{[k]} \\ 0 & 0 & -k\frac{E}{2(1+\nu)}\frac{h^{[k]3}}{12} \\ 0 & 0 & 0 \\ 0 & 0 & 0 \end{bmatrix}$$

$$\begin{bmatrix} 0 & 0 & 0 \\ 0 & 0 & 0 \\ -k\frac{E}{2(1+\nu)}\frac{h^{[k]3}}{12} & 0 & 0 \\ -k\frac{E}{2(1+\nu)}R^{[k]}\frac{h^{[k]3}}{12} & 0 & 0 \\ 0 & 0 & 0 \\ 0 & R^{[k]}\int_{-h^{[k]}/2}^{h^{[k]}/2} Kzdz & \int_{-h^{[k]}/2}^{h^{[k]}/2} Kz^3dz \end{bmatrix} \tag{30}$$

$$\left[A_2\right]=\begin{bmatrix} 0 & \frac{E(1-\nu)}{(1-2\nu)(1+\nu)}\frac{h^{[k]3}}{12} & 0 \\ -\frac{E(1-\nu)}{(1-2\nu)(1+\nu)}\frac{h^{[k]3}}{12} & -\frac{(1-\nu)}{(1-2\nu)(1+\nu)}\frac{h^{[k]2}}{12}\left(3R^{[k]}\frac{dh^{[k]}}{dx}+h^{[k]}\frac{dR^{[k]}}{dx}\right) & k\frac{E}{2(1+\nu)}R^{[k]}{}_h{}^{[k]} \\ 0 & -k\frac{E}{2(1+\nu)}R^{[k]}{}_h{}^{[k]} & -\frac{k}{2(1+\nu)}\left(R^{[k]}{}_E\frac{dh^{[k]}}{dx}+hE\frac{dR^{[k]}}{dx}\right) \\ 0 & \frac{E}{(1+\nu)}\frac{h^{[k]3}}{12}\left(\frac{2\nu}{(1-2\nu)}-\frac{k}{2}\right) & -\frac{kE}{2(1+\nu)}\frac{h^{[k]2}}{4}\frac{dh^{[k]}}{dx} \\ 0 & 0 & 0 \\ 0 & 0 & 0 \end{bmatrix}$$

$$\begin{bmatrix} 0 & 0 & 0 \\ \frac{E}{(1+\nu)}\frac{h[k]^3}{12}\left(\frac{k}{2}-\frac{\nu}{(1-2\nu)}\right) & \frac{E(1+\nu)}{(1-2\nu)(1+\nu)}\frac{h[k]^3}{12}\alpha & \frac{E(1+\nu)}{(1-2\nu)(1+\nu)}R\frac{h[k]^3}{12}\alpha \\ -\frac{kE}{2(1+\nu)}\frac{h[k]^2}{4}\frac{dh[k]}{dx} & 0 & 0 \\ -\frac{k}{2(1+\nu)}\frac{h[k]^2}{12}\left(h[k]_E\frac{dR[k]}{dx}+3R[k]_E\frac{dh[k]}{dx}\right) & 0 & 0 \\ 0 & 0 & 0 \\ 0 & \frac{dR[k]}{dx}\int_{-h[k]/2}^{h[k]/2} Kzdz & 0 \end{bmatrix} \tag{31}$$

$$\left[A_3\right]=\begin{bmatrix} \frac{E(1-\nu)}{(1-2\nu)(1+\nu)}R[k]_h[k] & 0 & \frac{E\nu}{(1-2\nu)(1+\nu)}h[k] \\ -\frac{E(1-\nu)}{(1-2\nu)(1+\nu)}\frac{h[k]^2}{4}\frac{dh[k]}{dx} & k\frac{E}{2(1+\nu)}R[k]_h[k] & 0 \\ \frac{E\nu}{(1-2\nu)(1+\nu)}h[k] & -\frac{kE}{2(1+\nu)}\left(R\frac{dh[k]}{dx}+h\frac{dR[k]}{dx}\right) & \frac{E(1-\nu)}{(1-2\nu)(1+\nu)}\ln\left(\frac{R+\frac{h[k]}{2}}{R-\frac{h[k]}{2}}\right) \\ \frac{E\nu}{(1-2\nu)(1+\nu)}R[k]_h[k] & -\frac{kE}{2(1+\nu)}\frac{h[k]^2}{4}\frac{dh[k]}{dx} & \frac{E}{(1-2\nu)(1+\nu)}\left(h[k]-(1-\nu)R[k]\ln\left(\frac{R[k]+\frac{h[k]}{2}}{R[k]-\frac{h[k]}{2}}\right)\right) \\ 0 & 0 & 0 \\ 0 & 0 & 0 \end{bmatrix}$$

$$\begin{bmatrix} \frac{E\nu}{(1-2\nu)(1+\nu)}R[k]_h[k] & -\frac{E(1+\nu)}{(1-2\nu)(1+\nu)}R[k]_h[k]_\alpha[k] & -\frac{E(1+\nu)}{(1-2\nu)(1+\nu)}\frac{h[k]^3}{12}\alpha[k] \\ \frac{E\nu}{(1-2\nu)(1+\nu)}\frac{h[k]^2}{2}\frac{dh[k]}{dx} & \frac{(1+\nu)}{(1-2\nu)(1+\nu)}\frac{h[k]^2}{12}\left(3\alpha[k]_E\frac{dh[k]}{dx}+h[k]_E\frac{d\alpha[k]}{dx}\right) & \frac{(1+\nu)}{(1-2\nu)(1+\nu)}\frac{h[k]^2}{12}\left(3\alpha[k]_{ER}[k]\frac{dh[k]}{dx}+h[k]_{ER}[k]\frac{d\alpha[k]}{dx}+\alpha[k]_{Eh}[k]\frac{dR[k]}{dx}\right) \\ -\frac{E}{(1-2\nu)(1+\nu)}\left(h[k]-(1-\nu)R[k]\ln\left(\frac{R[k]+\frac{h[k]}{2}}{R-\frac{h[k]}{2}}\right)\right) & -\frac{E(1+\nu)}{(1-2\nu)(1+\nu)}h[k]_\alpha[k] & 0 \\ \frac{E(1-\nu)}{(1-2\nu)(1+\nu)}R[k]^3\ln\left(\frac{R[k]+\frac{h[k]}{2}}{R[k]-\frac{h[k]}{2}}\right) & -\frac{E(1+\nu)}{(1-2\nu)(1+\nu)}R[k]_h[k]_\alpha[k] & -\frac{E(1+\nu)}{(1-2\nu)(1+\nu)}\frac{h[k]^3}{6}\alpha[k] \\ 0 & -R[k]\int_{-h[k]/2}^{h[k]/2} Kdz & -\int_{-h[k]/2}^{h[k]/2}\int_{-h[k]/2}^{h[k]/2} Kz^2dz \\ 0 & 0 & -\int_{-h[k]/2}^{h[k]/2} K(R+z)dz \end{bmatrix} \tag{32}$$

$$[F]=\begin{Bmatrix} C_1 \\ 0 \\ P\dfrac{h^{[k]}}{2}\left(R^{[k]}-\dfrac{h^{[k]}}{2}\right)+\dfrac{\rho\omega^2}{6}R^{[k]}h^{[k]^3} \\ -P\left(R^{[k]}-\dfrac{h^{[k]}}{2}\right)+\dfrac{\rho\omega^2}{6}\dfrac{h^{[k]}}{2}\left(12R^{[k]^2}+h^{[k]^2}\right) \\ \left[H_o\left(R^{[k]}-\dfrac{h^{[k]}}{2}\right)-H_i\left(R^{[k]}+\dfrac{h^{[k]}}{2}\right)\right]x+C_2 \\ \dfrac{h^{[k]}}{2}\left[H_i\left(R^{[k]}-\dfrac{h^{[k]}}{2}\right)+H_o\left(R^{[k]}+\dfrac{h^{[k]}}{2}\right)\right] \end{Bmatrix} \tag{33}$$

The elastic solution is completed by the application of the boundary and continuity conditions. Defining the differential operator $P(D)$, Eq. (28) is written as:

$$\begin{cases} \left[P(D)\right]^{[k]}=\left[B_1\right]^{[k]}D^2+\left[B_2\right]^{[k]}D+\left[B_3\right]^{[k]} \\ D^2=\dfrac{d^2}{dx^2}, \qquad D=\dfrac{d}{dx} \end{cases} \tag{34}$$

Thus

$$\left[P(D)\right]^{[k]}\{\bar{y}\}^{[k]}=\{F\}^{[k]} \tag{35}$$

The total solution of Eq. (35), is includes homogenous and particular parts. The homogeneous case is as follows:

$$\{y\}^{[k]}=\{y\}_h^{[k]}+\{y\}_p^{[k]} \tag{36}$$

Therefore, the total solution is as follows:

$$\begin{Bmatrix} U_x^{[k]} \\ U_z^{[k]} \end{Bmatrix}=\begin{Bmatrix} U_x^{[k]} \\ U_z^{[k]} \end{Bmatrix}_h+\begin{Bmatrix} U_x^{[k]} \\ U_z^{[k]} \end{Bmatrix}_p \qquad \left\{\theta^{[k]}\right\}=\left\{\theta^{[k]}\right\}_h+\left\{\theta^{[k]}\right\}_p \tag{37}$$

Then

$$\left\{U_x^{[k]},U_z^{[k]}\right\}=\sum_{i=1}^{6}C_i^{[k]}\{V\}_i^{[k]}e^{m_i^{[k]}x} \qquad \left\{T^{[k]}\right\}=\sum_{j=1}^{2}C_j^{T[k]}\{V\}_j^{T[k]}e^{m_j^{[k]}x} \tag{38}$$

In general state, the thermoelastic solution for each disk consists of 12 unknown values of $C_i^{[k]}, C_j^{T[k]}$ and an eight-order polynomial which are a six-order polynomial belonging to displacement and a two-order polynomial belonging to thermal. The result of the determinant above is completed by the application of the boundary and continuity conditions.

5. Boundary and Continuity Conditions

In this problem, the boundary conditions of the clamped-clamped cylindrical shell subjected to temperature are:

$$\begin{Bmatrix} u_0,u_1 \\ w_0,w_1 \\ \Theta^0 \\ \Theta^1 \end{Bmatrix}_{x=0}=\begin{Bmatrix} u_0,u_1 \\ w_0,w_1 \\ \Theta^0 \\ \Theta^1 \end{Bmatrix}_{x=L}=\begin{Bmatrix} 0 \\ 0 \\ T-T_{ref} \\ 0 \end{Bmatrix} \tag{39}$$

In the boundary between two layers, forces, stresses, and displacements are continuous due to the overall continuity and homogeneity in the cylinder. The continuity conditions are as follows:

$$\left\{\begin{matrix} U_x^{[k-1]}(x,z) \\ U_z^{[k-1]}(x,z) \end{matrix}\right\}_{x=x^{[k-1]}+\frac{t}{2}} = \left\{\begin{matrix} U_x^{[k]}(x,z) \\ U_z^{[k]}(x,z) \end{matrix}\right\}_{x=x^{[k]}-\frac{t}{2}} \tag{40}$$

$$\left\{\begin{matrix} U_x^{[k]}(x,z) \\ U_z^{[k]}(x,z) \end{matrix}\right\}_{x=x^{[k]}+\frac{t}{2}} = \left\{\begin{matrix} U_x^{[k+1]}(x,z) \\ U_z^{[k+1]}(x,z) \end{matrix}\right\}_{x=x^{[k+1]}-\frac{t}{2}} \tag{41}$$

And

$$\left\{\begin{matrix} \frac{dU_x^{[k-1]}(x,z)}{dx} \\ \frac{dU_z^{[k-1]}(x,z)}{dx} \end{matrix}\right\}_{x=x^{[k-1]}+\frac{t}{2}} = \left\{\begin{matrix} \frac{dU_x^{[k]}(x,z)}{dx} \\ \frac{dU_z^{[k]}(x,z)}{dx} \end{matrix}\right\}_{x=x^{[k]}-\frac{t}{2}} \tag{42}$$

$$\left\{\begin{matrix} \frac{dU_x^{[k]}(x,z)}{dx} \\ \frac{dU_z^{[k]}(x,z)}{dx} \end{matrix}\right\}_{x=x^{[k]}+\frac{t}{2}} = \left\{\begin{matrix} \frac{dU_x^{[k+1]}(x,z)}{dx} \\ \frac{dU_z^{[k+1]}(x,z)}{dx} \end{matrix}\right\}_{x=x^{[k+1]}-\frac{t}{2}} \tag{43}$$

According to the continuity conditions, in terms of z, T , 12 equations are obtained. In general, if the shell is divided into n disk layers, $12(n-1)$ equations are obtained. Utilizing the 12 equations of boundary condition, $12n$ equations are obtained. The solution of these equations yields $12n$ unknown constants.

6. Results and Discussion

The solution described in the preceding section for a homogeneous and isotropic cylindrical shell with variable thickness h , $h_1 = 40$ mm , $h_2 = 30$ mm , $R_1 = 100$ mm and $L = 1000$ mm will be considered. The Young's Modulus, Poisson's ratio, thermal expansion coefficient and thermal conductivity respectively, have values of $E = 200$ GPa , $\nu = 0.3$, $\alpha = 4.3\text{e-}6\ 1/^\circ C$ and $\kappa = 175\ W/\text{m}^\circ\text{C}$. The applied internal pressure is $P = 80$ MPa .The cylindrical rotates with $\omega = 500$ rad/s ,thermal loading is in the form of internal heat flux of $H_i = 150\ \text{W/m}^2$ and the boundary conditions for temperature are taken as $T_1 = 50\ ^\circ\text{C}$ and $T_2 = 50\ ^\circ\text{C}$ at the bottom and top of the cylinder. The cylindrical shell is subject to clamped-clamped boundary conditions, displacement and stresses are normalized by dividing it by the internal radii and internal pressure parameter, respectively.

In Figs. 3, displacement distributions obtained, using MLM, are compared with the solutions of FEM and are presented in the form of graph. It can be seen that this solution is in good agreement with verified FEM results. Fig. 3 shows the radial displacement along the cylinder for angular speed $\omega = 500$ rad/s . It is observed that at points far from the boundary, the radial displacement along the cylinder is almost uniform. In addition, the maximum amount of displacement distributions is related to the inner layer.

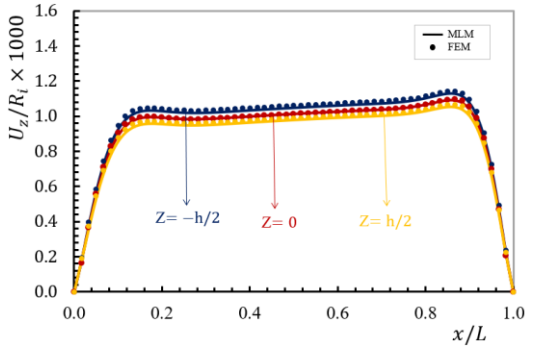

Fig. 3: Normalized radial displacement distribution in different layers ($\omega = 500 rad/s$)

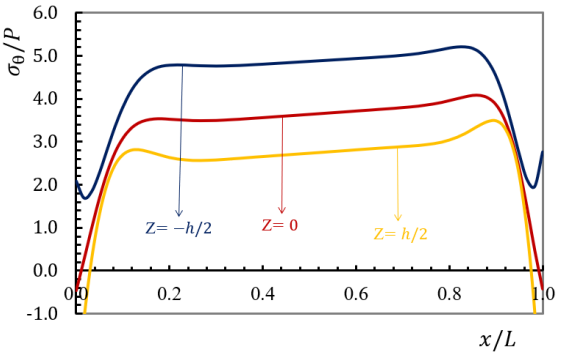

Fig. 4: Normalized circumferential stress distribution in different layers ($\omega = 500$ rad/s)

The distribution of circumferential stress at different layers is plotted in Fig. 4. It is observed that points far from the boundary are in a tensile state in all layers. Besides, at an arbitrary point along the length of the cylinder, the amount of circumferential stress is reduced from the inner layer to the outer layer.

In Fig. 5, the distribution of shear stress along the length of the cylinder is shown. As shown in the figure, shear stress can be ignored in all layers at points far from the boundary.

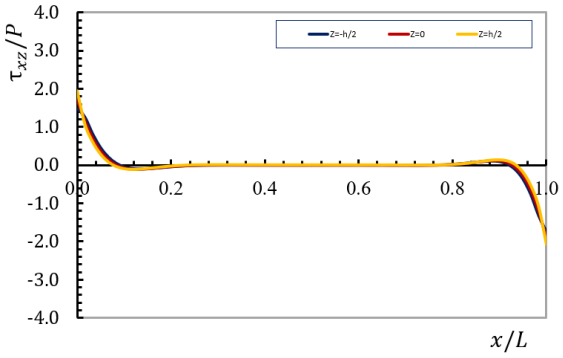

Fig. 5: Normalized shear stress distribution in different layers ($\omega = 500$ rad/s).

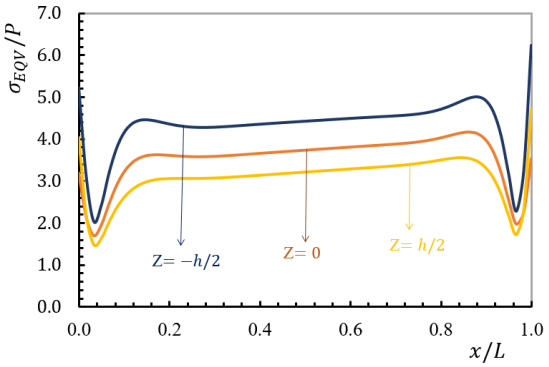

Fig. 6: Normalized equivalent stress distribution in different layers ($\omega = 500$ rad/s)

Fig. 6 shows the distribution of von Mises stress at different layers. It can be noted that at points away from boundaries, the von Mises stress is significant, especially on the internal surface, which is the greatest. It is observed that the amount of stress is in a tensile state in all layers

The effects of angular velocity ω on the distribution of the stresses and radial displacement in the middle layer are presented in Figs. 7-10. As shown in Fig. 7, increasing the amount of angular velocity has a significant effect on the amount of radial displacement. Also, compared to Fig. 3, the shape of the radial displacement profile remains almost unchanged.

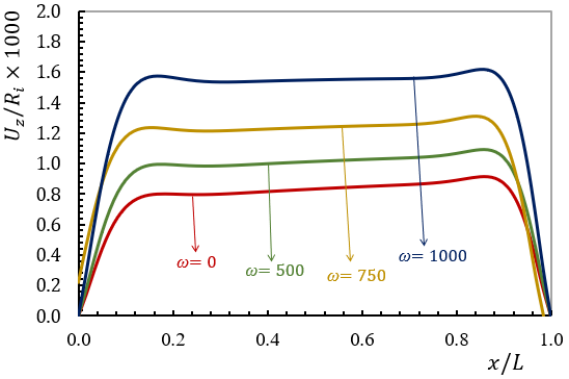

Fig. 7: Normalized radial displacement distribution subjected to different angular velocity ($h = 0$)

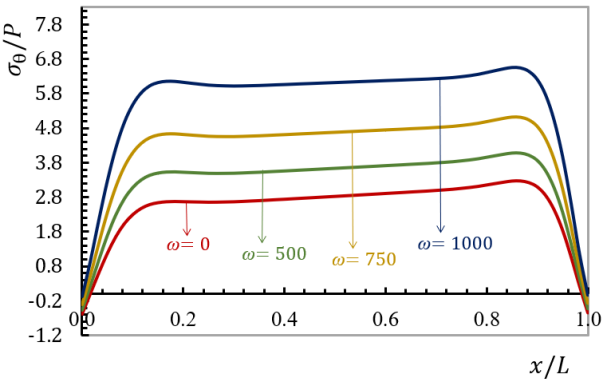

Fig. 8: Normalized circumferential stress distribution subjected to different angular velocity ($h = 0$).

Fig. 8 show the circumferential stress along the longitudinal direction in the middle layer at several angular velocities. As shown in the figure, the circumferential stress is of the tensile type and, like the displacement, the effect of angular velocity on the circumferential stress is significant and the shape of the profile remains almost unchanged.

In Fig. 9, the distribution of shear stress along the length of the cylinder at several angular velocities is shown. As shown in the figure, as in Fig. 5, the shear stress can be neglected in all layers at points away from the boundary, and the influence of the angular velocity on it is negligible.

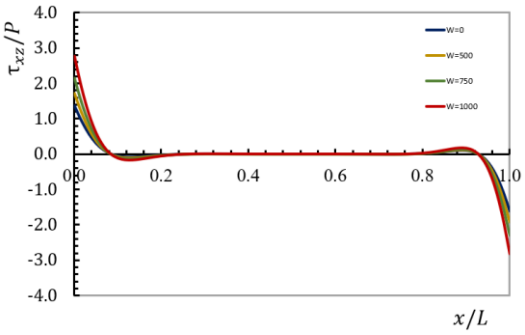

Fig. 9: Normalized shear stress distribution subjected to different angular velocity ($h = 0$).

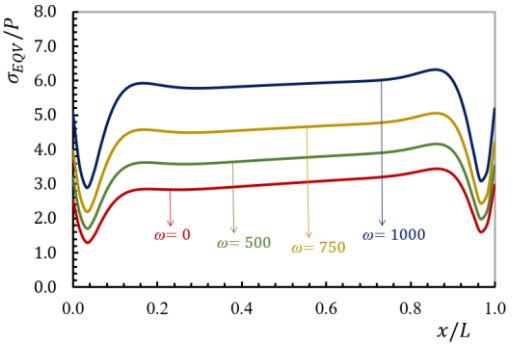

Fig. 10: Normalized equivalent stress distribution subjected to different angular velocity ($h = 0$).

distribution of von Mises stress at different layers along the length of the cylinder at several angular velocities are shown in Fig. 10. As the angular velocity increases, the von Mises stress also increases.

7. Conclusions

This paper aims to develop analytical formulations and solutions for isotropic rotating thick-walled cylindrical pressure vessels with variable thickness, subjected to internal pressure and thermal loading, using FSDT. The basic equations for cylindrical shells with variable thickness are derived and solved using MLM, with clamped-clamped boundary conditions. The results for stresses and displacements are compared with those obtained through FEM solutions, and good agreement is found between them. The effects of varying angular velocities of the cylinder within a certain range on stresses and displacements are investigated.

The obtained results demonstrate that the maximum value of von Mises stresses due to mechanical and thermal loading in cylinders with variable thickness under clamped-clamped conditions occurs near the boundaries. It is also noted that with increasing angular velocities within the investigated range, radial displacement and von Mises stress increase at points away from the boundaries.

References

[1] P. Fatehi, M. Z. Nejad, Effects of material gradients on onset of yield in FGM rotating thick cylindrical shells, *International Journal of Applied Mechanics,* Vol. 6, No. 4, pp. 1450038, 2014.

[2] Z. Mazarei, M. Z. Nejad, A. Hadi, Thermo-elasto-plastic analysis of thick-walled spherical pressure vessels made of functionally graded materials, *International Journal of Applied Mechanics,* Vol. 8, No. 4, pp. 1650054, 2016.

[3] M. Z. Nejad, M. Jabbari, A. Hadi, A review of functionally graded thick cylindrical and conical shells, *Journal of Computational Applied Mechanics,* Vol. 48, No. 2, pp. 357-370, 2017.

[4] A. Farajpour, A. Rastgoo, Size-dependent static stability of magneto-electro-elastic CNT/MT-based composite nanoshells under external electric and magnetic fields, *Microsystem Technologies,* Vol. 23, pp. 5815-5832, 2017.

[5] T. Ebrahimi, M. Z. Nejad, H. Jahankohan, A. Hadi, Thermoelastoplastic response of FGM linearly hardening rotating thick cylindrical pressure vessels, *Steel and Composite Structures, An International Journal*, Vol. 38, No. 2, pp. 189-211, 2021.

[6] A. Afshin, M. Z. Nejad, K. Dastani, Transient thermoelastic analysis of FGM rotating thick cylindrical pressure vessels under arbitrary boundary and initial conditions, *Journal of Computational Applied Mechanics,* Vol. 48, No. 1, pp. 15-26, 2017.

[7] M. Kashkoli, K. N. Tahan, M. Z. Nejad, Time-dependent creep analysis for life assessment of cylindrical vessels using first order shear deformation theory, *Journal of Mechanics,* Vol. 33, No. 4, pp. 461-474, 2017.

[8] M. Gharibi, M. Z. Nejad, A. Hadi, Elastic analysis of functionally graded rotating thick cylindrical pressure vessels with exponentially-varying properties using power series method of Frobenius, *Journal of Computational Applied Mechanics,* Vol. 48, No. 1, pp. 89-98, 2017.

[9] M. Z. Nejad, T. Taghizadeh, S. J. Mehrabadi, S. Herasati, Elastic analysis of carbon nanotube-reinforced composite plates with piezoelectric layers using shear deformation theory, *International Journal of Applied Mechanics,* Vol. 9, No. 1, pp. 1750011, 2017.

[10] M. D. Kashkoli, K. N. Tahan, M. Z. Nejad, Time-dependent thermomechanical creep behavior of FGM thick hollow cylindrical shells under non-uniform internal pressure, *International Journal of Applied Mechanics,* Vol. 9, No. 6, pp. 1750086, 2017.

[11] M. Jabbari, M. Z. Nejad, Mechanical and thermal stresses in radially functionally graded hollow cylinders with variable thickness due to symmetric loads, *Australian Journal of Mechanical Engineering*, Vol. 18, pp. 108-121, 2020.

[12] M. H. Dindarloo, L. Li, Vibration analysis of carbon nanotubes reinforced isotropic doubly-curved nanoshells using nonlocal elasticity theory based on a new higher order shear deformation theory, *Composites Part B-Engineering,* Vol. 175, pp. 107170, 2019.

[13] T. Taghizadeh, M. Z. Nejad, M. D. Kashkoli, Thermo-elastic creep analysis and life assessment of thick truncated conical shells with variable thickness, *International Journal of Applied Mechanics,* Vol. 11, No. 9, pp. 1950086, 2019.

[14] A. H. Sofiyev, F. Dikmen, Buckling analysis of functionally graded shells under mixed boundary conditions subjected to uniform lateral pressure, *Journal of Applied and Computational Mechanics,* Vol. 7, No. 1, pp. 345-354, 2021.

[15] T. Taghizadeh, M. Z. Nejad, Thermo-elastic creep analysis and life assessment of rotating thick pressurized cylindrical shells using third-order shear deformation theory, *Journal of Computational Applied Mechanics,* Vol. 52, No. 3, pp. 366-393, 2021.

[16] M. Jabbari, M. Z. Nejad, Electro-mechanical analysis of rotating cylinder made of functionally graded piezoelectric materials: Sensor and actuator, *Amirkabir Journal of Mechanical Engineering,* Vol. 51, No. 1, pp. 215-224, 2019.

[17] M. D. Kashkoli, K. N. Tahan, M. Z. Nejad, Creep damage and life assessment of thick cylindrical pressure vessels with variable thickness made of 304L austenitic stainless steel, *Steel and Composite Structures, An International Journal*, Vol. 32, No. 6, pp. 701, 2019.

[18] M. Z. Nejad, Z. Hoseini, A. Niknejad, M. Ghannad, Steady-state creep deformations and stresses in FGM rotating thick cylindrical pressure vessels, *Journal of Mechanics,* Vol. 31, No. 1, pp. 1-6, 2015.

[19] M. D. Kashkoli, M. Z. Nejad, Time-dependent thermo-elastic creep analysis of thick-walled spherical pressure vessels made of functionally graded materials, *Journal of Theoretical and applied Mechanics,* Vol. 53, No. 4, pp. 1053-1065, 2015.

[20] M. Z. Nejad, P. Fatehi, Exact elasto-plastic analysis of rotating thick-walled cylindrical pressure vessels made of functionally graded materials, *International Journal of Engineering Science,* Vol. 86, pp. 26-43, 2015.

[21] M. Z. Nejad, M. D. Kashkoli, Time-dependent thermo-creep analysis of rotating FGM thick-walled cylindrical pressure vessels under heat flux, *International Journal of Engineering Science,* Vol. 82, pp. 222-237, 2014.

[22] M. Dehghan, M. Z. Nejad, A. Moosaie, Thermo-electro-elastic analysis of functionally graded piezoelectric shells of revolution: Governing equations and solutions for some simple cases, *International Journal of Engineering Science,* Vol. 104, pp. 34-61, 2016.

[23] M. D. Kashkoli, M. Z. Nejad, Time-dependent creep analysis and life assessment of 304 L austenitic stainless steel thick pressurized truncated conical shells, *Steel and Composite Structures, An International Journal,* Vol. 28, No. 3, pp. 349-362, 2018.

[24] M. Z. Nejad, N. Alamzadeh, A. Hadi, Thermoelastoplastic analysis of FGM rotating thick cylindrical pressure vessels in linear elastic-fully plastic condition, *Composites Part B-Engineering,* Vol. 154, pp. 410-422, 2018.

[25] A. Farajpour, A. Rastgoo, M. Farajpour, Nonlinear buckling analysis of magneto-electro-elastic CNT-MT hybrid nanoshells based on the nonlocal continuum mechanics, *Composite Structures,* Vol. 180, pp. 179-191, 2017.

[26] L. Li, X. Li, Y. Hu, Nonlinear bending of a two-dimensionally functionally graded beam, *Composite Structures,* Vol. 184, pp. 1049-1061, 2018.

[27] M. Z. Nejad, G. H. Rahimi, M. Ghannad, Set of field equations for thick shell of revolution made of functionally graded materials in curvilinear coordinate system, *Mechanika,* Vol. 77, No. 3, pp. 18-26, 2009.

[28] M. Ghannad, M. Z. Nejad, Elastic analysis of pressurized thick hollow cylindrical shells with clamped-clamped ends, *Mechanika,* Vol. 85, No. 5, pp. 11-18, 2010.

[29] Y.-W. Zhang, G.-L. She, Nonlinear primary resonance of axially moving functionally graded cylindrical shells in thermal environment, *Mechanics of Advanced Materials and Structures*, pp. 1-13, 2023.

[30] I. Panferov, Stresses in a transversely isotropic conical elastic pipe of constant thickness under a thermal load, *Journal of Applied Mathematics and Mechanics,* Vol. 56, No. 3, pp. 410-415, 1992.

[31] B. Sundarasivarao, N. Ganesan, Deformation of varying thickness of conical shells subjected to axisymmetric loading with various end conditions, *Engineering Fracture Mechanics,* Vol. 39, No. 6, pp. 1003-1010, 1991.

[32] I. Mirsky, G. Herrmann, Axially symmetric motions of thick cylindrical shells, *Journal of Applied Mechanics,* Vol. 25, No. 1, 97-102, 1958.

[33] F. Witt, Thermal stress analysis of conical shells, *Nuclear Structural Engineering,* Vol. 1, No. 5, pp. 449-456, 1965.

[34] K. Jane, Y. Wu, A generalized thermoelasticity problem of multilayered conical shells, *International Journal of Solids and Structures,* Vol. 41, No. 9-10, pp. 2205-2233, 2004.

[35] H. R. Eipakchi, S. Khadem, G. H. Rahimi, Axisymmetric stress analysis of a thick conical shell with varying thickness under nonuniform internal pressure, *Journal of Engineering Mechanics,* Vol. 134, No. 8, pp. 601-610, 2008.

[36] M. Ghannad, M. Z. Nejad, G. H. Rahimi, Elastic solution of axisymmetric thick truncated conical shells based on first-order shear deformation theory, *Mechanika,* Vol. 79, No. 5, pp. 13-20, 2009.

[37] M. Arefi, G. Rahimi, Thermo elastic analysis of a functionally graded cylinder under internal pressure using first order shear deformation theory, *Scientific Research and Essays,* Vol. 5, No. 12, pp. 1442-1454, 2010.

[38] H. R. Eipakchi, Third-order shear deformation theory for stress analysis of a thick conical shell under pressure, *Journal of Mechanics of Materials and Structures,* Vol. 5, No. 1, pp. 1-17, 2010.

[39] M. Ghannad, G. H. Rahimi, M. Z. Nejad, Determination of displacements and stresses in pressurized thick cylindrical shells with variable thickness using perturbation technique, *Mechanika,* Vol. 18, No. 1, pp. 14-21, 2012.

[40] Ö. Civalek, Vibration analysis of laminated composite conical shells by the method of discrete singular convolution based on the shear deformation theory, *Composites Part B-Engineering,* Vol. 45, No. 1, pp. 1001-1009, 2013.

[41] M. Z. Nejad, M. Jabbari, M. Ghannad, Elastic analysis of rotating thick truncated conical shells subjected to uniform pressure using disk form multilayers, *International Scholarly Research Notices,* Vol. 2014, 2014.

[42] M. Z. Nejad, M. Jabbari, M. Ghannad, A semi-analytical solution of thick truncated cones using matched asymptotic method and disk form multilayers, *Archive of Mechanical Engineering,* Vol. 61, No. 3, pp. 495--513, 2014.

[43] M. Ghannad, G. H. Rahimi, M. Z. Nejad, Elastic analysis of pressurized thick cylindrical shells with variable thickness made of functionally graded materials, *Composites Part B-Engineering,* Vol. 45, No. 1, pp. 388-396, 2013.

[44] M. Z. Nejad, M. Jabbari, M. Ghannad, Elastic analysis of rotating thick cylindrical pressure vessels under non-uniform pressure: linear and non-linear thickness, *Periodica Polytechnica Mechanical Engineering,* Vol. 59, No. 2, pp. 65-73, 2015.

[45] M. Ghannad, M. Jabbari, M. Z. Nejad, An elastic analysis for thick cylindrical pressure vessels with variable thickness, *Engineering Solid Mechanics,* Vol. 3, No. 2, pp. 117-130, 2015.

[46] L. Xin, G. Dui, S. Yang, D. Zhou, Solutions for behavior of a functionally graded thick-walled tube subjected to mechanical and thermal loads, *International Journal of Mechanical Sciences,* Vol. 98, pp. 70-79, 2015.

[47] H. Gharooni, M. Ghannad, M. Z. Nejad, Thermo-elastic analysis of clamped-clamped thick FGM cylinders by using third-order shear deformation theory, *Latin American Journal of Solids and Structures,* Vol. 13, pp. 750-774, 2016.

[48] M. Jabbari, M. Z. Nejad, M. Ghannad, Thermo-elastic analysis of axially functionally graded rotating thick cylindrical pressure vessels with variable thickness under mechanical loading, *International Journal of Engineering Science,* Vol. 96, pp. 1-18, 2015.

[49] M. Z. Nejad, M. Jabbari, M. Ghannad, Elastic analysis of axially functionally graded rotating thick cylinder with variable thickness under non-uniform arbitrarily pressure loading, *International Journal of Engineering Science,* Vol. 89, pp. 86-99, 2015.

[50] M. Jabbari, M. Z. Nejad, M. Ghannad, Thermoelastic analysis of rotating thick truncated conical shells subjected to non-uniform pressure, *Journal of Solid Mechanics*, Vol. 8, No. 3, pp. 466-481, 2016.

[51] M. Jabbari, M. Z. Nejad, M. Ghannad, Thermo-elastic analysis of axially functionally graded rotating thick truncated conical shells with varying thickness, *Composites Part B-Engineering,* Vol. 96, pp. 20-34, 2016.

[52] M. Ghannad, M. Z. Nejad, Elastic solution of pressurized clamped-clamped thick cylindrical shells made of functionally graded materials, *Journal of Theoretical and Applied Mechanics,* Vol. 51, No. 4, pp. 1067-1079, 2013.

[53] M. Jabbari, M. Z. Nejad, M. Ghannad, Stress analysis of rotating thick truncated conical shells with variable thickness under mechanical and thermal loads, *Journal of Solid Mechanics,* Vol. 9, No. 1, pp. 100-114, 2017.

[54] A. Yasinskyy, L. Tokova, Inverse problem on the identification of temperature and thermal stresses in an FGM hollow cylinder by the surface displacements, *Journal of Thermal Stresses,* Vol. 40, No. 12, pp. 1471-1483, 2017.

[55] M. Z. Nejad, M. Jabbari, M. Ghannad, A general disk form formulation for thermo-elastic analysis of functionally graded thick shells of revolution with arbitrary curvature and variable thickness, *Acta Mechanica,* Vol. 228, pp. 215-231, 2017.

[56] A. A. Hamzah, H. K. Jobair, O. I. Abdullah, E. T. Hashim, L. A. Sabri, An investigation of dynamic behavior of the cylindrical shells under thermal effect, *Case Studies in Thermal Engineering,* Vol. 12, pp. 537-545, 2018.

[57] M. D. Kashkoli, K. N. Tahan, M. Z. Nejad, Thermomechanical creep analysis of FGM thick cylindrical pressure vessels with variable thickness, *International Journal of Applied Mechanics,* Vol. 10, No. 1, pp. 1850008, 2018.

[58] F. Aghaienezhad, R. Ansari, M. Darvizeh, On the stability of hyperelastic spherical and cylindrical shells subjected to external pressure using a numerical approach, *International Journal of Applied Mechanics,* Vol. 14, No. 10, pp. 2250094, 2022.

[59] O. Ifayefunmi, D. Ruan, Buckling of stiffened cone–cylinder structures under axial compression, *International Journal of Applied Mechanics,* Vol. 14, No. 7, pp. 2250075, 2022.
[60] M. Y. Ariatapeh, M. Shariyat, M. Khosravi, Semi-analytical large deformation and three-dimensional stress analyses of pressurized finite-length thick-walled incompressible hyperelastic cylinders and pipes, *International Journal of Applied Mechanics,* Vol. 15, No. 1, pp. 2250100, 2023.
[61] M. Z. Nejad, M. Jabbari, M. Ghannad, Elastic analysis of FGM rotating thick truncated conical shells with axially-varying properties under non-uniform pressure loading, *Composite Structures,* Vol. 122, pp. 561-569, 2015.
[62] S. Mannani, L. Collini, M. Arefi, Mechanical stress and deformation analyses of pressurized cylindrical shells based on a higher-order modeling, *Defence Technology,* Vol. 20, pp. 24-33, 2023.
[63] J. N. Reddy, *Theory and analysis of elastic plates and shells*, second edition, CRC press, USA, 2006.
[64] A. P. Boresi, R. J. Schmidt, O. M. Sidebottom, *Advanced mechanics of materials*, fifth edition, John Wiley & Sons, New York, 1993.
[65] M. Ghannad, M. P. Yaghoobi, 2D thermo elastic behavior of a FG cylinder under thermomechanical loads using a first order temperature theory, *International Journal of Pressure Vessels and Piping,* Vol. 149, pp. 75-92, 2017.
[66] K. Mohammadi, M. Mahinzare, K. Ghorbani, M. Ghadiri, Cylindrical functionally graded shell model based on the first order shear deformation nonlocal strain gradient elasticity theory, *Microsystem Technologies,* Vol. 24, pp. 1133-1146, 2018.
[67] A. C. Ugural, *Stresses in beams, plates, and shells*, third edition, CRC press, USA, 2010.
[68] S. Vlachoutsis, Shear correction factors for plates and shells, *International Journal for Numerical Methods in Engineering*, Vol. 33, No. 7, pp. 1537-1552, 1992.